

## Flow and Turbulent Processes in the Coastal Ocean

G. N. Ivey

School of Civil, Environmental and Mining Engineering & UWA Oceans Institute,  
University of Western Australia, Crawley, Western Australia 6008, Australia.

### Abstract

The coastal ocean is of great importance due to the proximity of coastal population centres, industry activity in the region ranging from fishing to tourism and the ever-growing offshore developments of the energy industry, particularly in the Australian North West Shelf (NWS) which is a focus area in this paper. The NWS is a particularly energetic portion of the coastal ocean, stirred by strong tides and aperiodic tropical cyclones in the summer months. Management of these coastal ocean regions requires quantitative process understanding hence and ocean forecasting capability of the coastal ocean dynamics. Here we focus on the two key issues for the NWS: the occurrence and predictability of the internal tide, and the assessment of ocean turbulence driven by this dominant forcing process.

### Introduction

The coastal ocean regions are of immense importance in terms of both economic and environmental significance. In Australia, the offshore oil and gas industry is currently constructing \$120 billion in projects on the NWS alone [11] and industry is expanding into deeper waters, including the Great Australian Bight. These coastal regions are also home to unique marine environments, typified by areas such as the UN World Heritage site at Ningaloo Reef, Western Australia. Knowledge of the mean and turbulent state of the ocean is essential for engineering design of offshore structures, for safe and reliable marine operations, and also environmental management of the marine ecosystems in the coastal ocean.

The NWS region is one of the most energetic coastal ocean regions in the world. It is forced by strong tides, ranging up to 10 m in amplitude in the Kimberley region, and cyclones in the summer season. While there is little fresh water input, the strong solar heating ensures strong vertical density stratification due to temperature throughout the year. The large-amplitude tides, in combination with this stratification and sloping offshore bathymetry, generate some of the strongest internal tides - internal waves at the tidal period - in the global ocean [8, 25]. As these waves propagate inshore they steepen and break, in turn, creating intense turbulent mixing and enhanced bottom stresses [22].

Offshore engineering infrastructure includes a labyrinth of bottom pipelines, often long pipelines taking gas to either shore-based Liquefied Natural Gas (LNG) plants, fixed offshore platforms or floating offshore facilities. From an engineering point of view, there are many key questions that are important. What is the time-dependency and intensity of the mean flow expected at any given location and hence what is the loading on engineering structures? What is the turbulence intensity over the entire water column induced by these time-dependent mean flows? What are the properties of the near-bottom flows and, in particular, the induced bottom stress and potential for sediment transport and scour? Many of these questions relate to extreme event prediction. From an environmental management point of

view, the overall goals relate to ensuring that developments operate in a safe and reliable manner with quantifiable and minimal environmental impact.

With these questions in mind, and with particular focus on the Australian North West Shelf, in this paper we examine two aspects of this problem: the prediction of the internal tide and the turbulent processes forced by the internal tide.

### Internal Waves Driven by the Tide

Internal waves in the ocean can be generated by large-scale pressure systems, by wind or by the mean flow interacting with topography [25, 26, 27]. In the ocean, the dominant generation mechanism is due to the mean flow associated with the tidally forced movement of the free surface, in turn, generating an oscillating horizontal mean flow over the entire water column at the local forcing tidal period. Typically the lunar M2 tide with period 12.4 h is the most important [8, 25, 26]. This oscillating tidal flow forces density-stratified water over the sloping bottom topography, creating internal pressure gradients and thus producing internal waves which radiate obliquely away from the bottom generation site in the form of beams. Such waves are known as internal tides [26]. Internal tides are generated, and later dissipated, at preferential locations or critical points whose location depends on the relative values of the local bottom slope, tidal frequency and density stratification [16]. As the internal waves propagate through the ocean they can be described in terms of both beam and modal descriptions [24, 26]. The propagation is further influenced by the background circulation and stratification, which varies spatially and seasonally in the upper layers, and the combined effect of these processes creates a rich and complex internal wave field in the ocean [12].

As the amplitude of the internal wave increases, nonlinear effects start to become important. When the propagating internal tide has moved into shallower water, it has more of a mode-like character and propagates horizontally on the seasonal thermocline. The overall density stratification inshore can be approximated by a two-layer density structure. This leads to new classes of waves, often referred to as solitons in the literature [23], but which are best described as nonlinear internal waves of large amplitude (NLIWs). NLIW's are seen throughout the global ocean [10] and, as they propagate, they induce large vertical displacements of constant density (isopycnal) surfaces of  $O(100\text{ m})$  and strong horizontal velocities of  $O(1-2\text{ ms}^{-1})$  [25]. Such large displacements and velocities, in turn, affect nutrient mixing and biological productivity [13], sediment resuspension [22]; the propagation of acoustic waves, and is of particular interest for marine and offshore engineering operations [20].

Consider the wave in the simple two-layer density stratification shown in Figure 1. The initially small amplitude linear long wave shown can progressively steepen due to non-linear effects [2]. Eventually dispersive effects, which tend to flatten the wave, become important and balance the steepening process and this

combination of effects is described by the Korteweg-de Vries (KdV) equation [23]

$$\eta_t + c_0 \eta_x + \alpha \eta \eta_x + \beta \eta_{xxx} = 0 \quad (1)$$

where

$$c_0 = \sqrt{\frac{g \Delta \rho}{\rho_1} \frac{h_1 h_2}{h_1 + h_2}} \quad (2)$$

$$\alpha = \frac{3}{2} c_0 \frac{(h_1 - h_2)}{h_1 h_2} \quad (3)$$

$$\beta = \frac{1}{6} c_0 h_1 h_2 \quad (4)$$

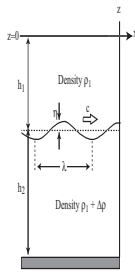


Fig.3(a)

Figure 1. Schematic of a two-layer density stratification with an internal wave propagating at the interface.

where (2) is the wave speed, (3) describes the self-steepening effects, and (4) the dispersive effects.

Analytical solutions of equation (1) can be found for a broad range of circumstances [23], including the classical hump-shaped solitary wave  $\eta = a \operatorname{sech}^2((x-ct)/L)$ , where the lengthscale

$L = (\beta/12a\alpha)^{1/2}$  and the wave propagates at a speed dependent

upon the wave amplitude  $a$  given by  $c = c_0(1 + 0.33\alpha a)$ . KdV theory and its weakly nonlinear relatives are, however, restricted to waves with small amplitude compared to the shallow layer depth (in the ocean usually  $h_1 < h_2$ ). However, many oceanic internal waves have amplitudes greater than the shallow layer depth and when solitary waves shoal, and overturning and turbulent breaking occurs (see below), a combination of laboratory experiments [25], direct field observations [17] and fully nonlinear and nonhydrostatic numerical simulations [27] must instead be used to describe the motion.

Despite these complexities, this would nevertheless suggest a quantity as fundamental as the arrival of an internal tide at a particular location should be quite predictable: if the semidiurnal M2 tide is the dominant tidal constituent, then every 12.4 h a new wave will arrive and it will be travelling at speed  $c$  (presumably greater than the linear internal wave speed given by (2)). Observations from the North Rankin A gas platform on the NWS [25] have shown the observed wave speeds can be as much as twice the linear wave speed given by (1). But what is surprising is that up to *three* waves can arrive at the platform in one 12.4 h tidal period.

To investigate this, a fully non-hydrostatic model simulation of the generation and propagation of NLIWs in the region has been undertaken. The model is the SUNTANS model [6], and in this set-up horizontal resolution was 50m in the horizontal with 200 layers in the vertical and 5 s timestep, and forcing is pure M2 tide at the offshore boundary [7]. As seen in Figure 2, a number of features are evident: the internal tide is generated offshore on the continental slope in depths of approximately 700 m; the internal tidal beam propagates shoreward from this site; the beam bends towards the horizontal in response to the strengthening density stratification at depths less than 400 m; and inshore there are essentially horizontally propagating “shock-like” features in water of 200 m and less.

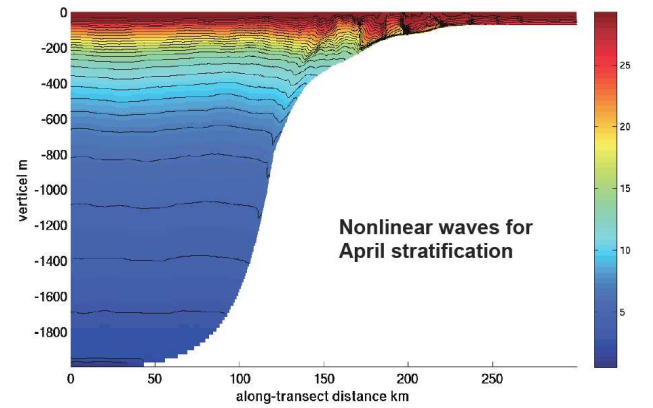


Figure 2. Sample output from SUNTANS showing cross-section perpendicular to the coast (colour scale is temperature in degC) from [7].

At a fixed location in shallow water at 125 m water depth in the domain shown in Figure 2, a time series of observed isotherm displacements is shown in Figure 3. Clearly visible are the large amplitude shock-like waves, with isotherms descending from about -20m to -80m in minutes, demonstrating why fully non-hydrostatic models are needed to describe this type of phenomena. Note also there are three wave fronts coming by the fixed location in timescales of 12 h.

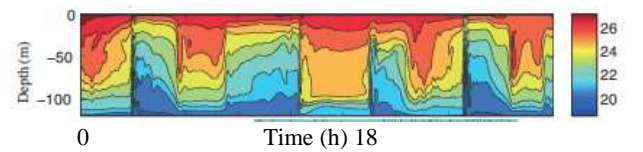


Figure 3. Times series of isotherm displacements, at the 125m depth location in Figure 2, from the SUNTANS simulations [7].

The key difference between the simulation and the assumptions underlying the use of an analytic solution like (1), for example, is the background velocity field in the simulation (or ocean) is non-zero. Specifically, the total velocity in the simulations is always the superposition of the induced velocity field associated with the propagating internal tide (i.e. the baroclinic motion) and the background velocity field associated with the (forcing) barotropic tide. The wave packets will have a velocity  $c$  that, although varying with depth and time as the wave amplitude increases due to the action of the self-steepening term (3), is always directed towards shallow water. On the other hand, the background tidal flow will have a depth-independent velocity given by  $U_B = U_0 \sin \omega t$ , where the tidal period  $T = (2\pi/\omega) = 12.4$  h. Clearly the quantity  $U_B < 0$  every half-cycle during the ebb phase of the tide and is thus in the opposite direction to wave speed  $c$ . As we move into shallower water and, ignoring turbulent

dissipation for the moment (see below), mass conservation requires  $U_0$  to increase. The key parameter is the Froude number  $Fr = c/|U_B|$ . When locally  $Fr = 1$ , and the tidal flow is directed offshore, then the incoming wave can be (temporarily) arrested. When locally  $Fr < 1$ , and the tidal flow is directed offshore, then the incoming wave can actually move backwards and offshore in an Eulerian reference frame. The scenarios are summarized in Figure 4.

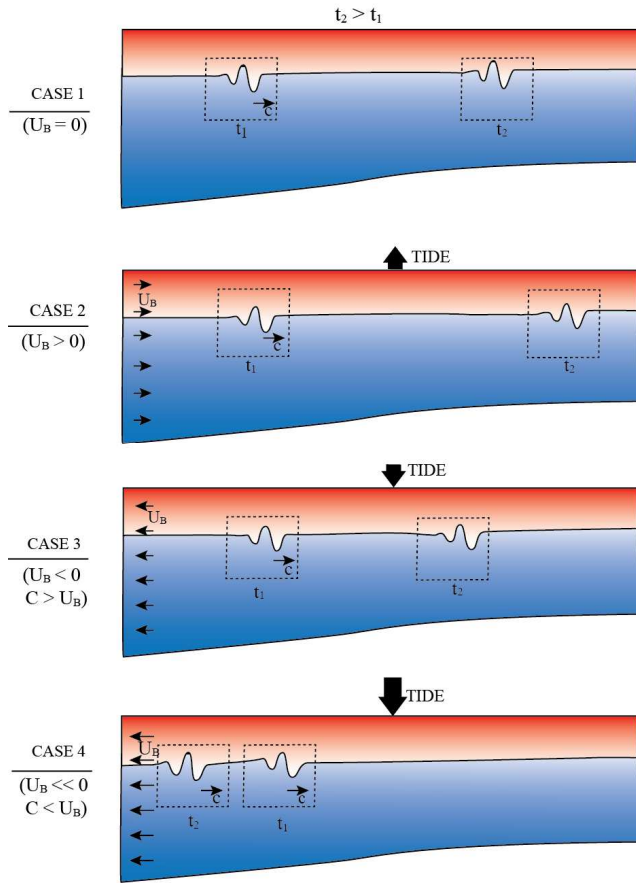


Figure 4. Schematics of a right-propagating wave moving towards shallow water in four cases with different intensity of the background flow  $U_B$ . In case 4,  $Fr < 1$  and the wave moves backwards in an Eulerian frame.  $t_2 > t_1$  in all cases.

Detailed calculation of the velocity components shows the situation in Figure 3 is one where the incoming wave first moves inshore, then as the tide reverses and the local  $Fr < 1$  it is swept back offshore (note the structure of the wave is mirrored as the tail passes the observation point first). As the tide subsequently reverses and flows onshore again, the wave then sweeps by for a third and final time, at a speed equal to the sum of  $c$  and  $U_B$ . Note the wave is continually evolving under the internal self-steepening effects, and the time the wave takes to pass a point is always the product of the local wavelength and the total speed, and both change with time. The first is changing relatively slowly in time, the second is rapidly changing in time, and hence the same wave can appear to be “compressed” or “expanded” at the observation site. The main point is there is only one wave packet, it simply passes the same observation point three times as it goes by in different directions!

## Turbulent Processes and the Internal Tide

The internal tidal dynamics described above are clearly highly unsteady and thus turbulent processes forced by these mean flows are also highly unsteady. When the amplitude of a NLIW becomes significant with respect to the total water depth, the leading edge of the wave steepens and the trailing edge flattens, transforming the wave into an upslope internal bore; the wave breaks, and this process is likely important not only locally but also to global ocean mixing [19]. To characterize this solitary wave breaking process, [2] introduced the Iribarren number

$$Ir = \frac{s}{\sqrt{a/L}} \quad (5)$$

where  $s$  is the bottom slope. While [2] only considered waves described by KdV theory, [24] extended this to very large amplitude NLIWs with amplitudes larger than the upper layer depth and, depending on the value of  $Ir$ , defined the five possible regimes shown in Figure 5. As the waves approach the slope,

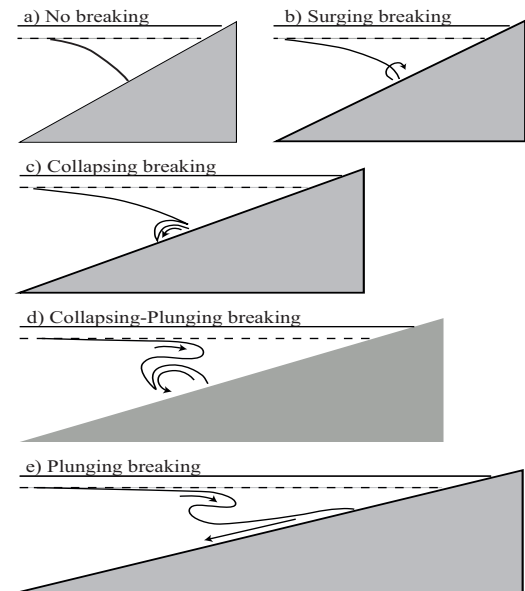


Figure 4

Figure 5. Schematic of NLIW breaking regimes from [25] where the dotted line delineates the undisturbed density interface in this two-layer approximation.

there is a drawdown of the density interface along the bottom from the rest position and [24] found the maximum extent of this interface drawdown was given by  $H_i \propto \sqrt{4saL}$ . This drawdown depth can be up to 200 m and corresponding excursion lengths along the bottom slope can be as much as 5 km. Considerable portions of the coastal ocean can thus be influenced by direct interaction with breaking NLIWs, and breaking NLIWs can lead to near bed velocities in excess of  $1 \text{ m s}^{-1}$  [25], strongly vertically sheared currents [17] and enhanced mixing [4,14].

In engineering design the practice is to typically double the factor of safety for any bottom infrastructure in these regions. The prediction of sediment mobilization is also critical to the design and operation of offshore infrastructure, and NLIWs can contribute to and even dominate the resuspension and transport of sediment on continental slopes and shelves, and can even shape

the continental slope and shelf on geologic time scales [5]. When NLIWs shoal, numerical modeling and laboratory experiments have determined that global instabilities form in the turbulent boundary layer [1]. The highly energetic content of the associated coherent vortical structures (including the height obtained when they are ejected from the bed) appears to be the driving mechanism for sediment resuspension and entrainment under shoaling NLIWs [1].

The shoaling process is highly non-stationary and must be taken into account when modelling re-suspension. This indicates traditional steady near-bed viscous stress models must be used with caution, and rather approaches that are able to estimate the instantaneous bed shear stress are called for. Recently, [18] have demonstrated an approach developed from the wind tunnel, atmospheric boundary layer and associated DNS calculations can be extended to aquatic environments. In particular, the instantaneous bottom shear stress can be estimated from single point measurements taken in the log layer. The field data in [18] was taken in a tidal estuary, and the next step is to apply this to the ocean bottom boundary layer. The direct measurement of bottom stress is not possible in field situations and this approach offers a unique way to quantify not only the process of sediment re-suspension and transport but to quantify benthic nutrient fluxes into the water column, estimates needed in ecological models, for example [28].

Above the relatively thin and well-mixed bottom boundary layer, the effects of the overlying stable density stratification start to become significant in influencing the turbulence and mixing characteristics. Quantifying the vertical turbulent fluxes in the density-stratified ocean water column is key to assessing fluxes of heat and nutrients to/from the surface and bottom boundary layers. It is also important in characterising the ambient mean flow and turbulence characteristics for engineering structural design. Despite decades of measurements on the NWS, mainly by the oil and gas companies, of mean flows driven by tides and internal waves principally, until 2012 there had been no measurements of the turbulent microstructure on the NWS. In the ocean, it is extremely difficult to measure turbulent fluxes directly, and common practice is thus to measure the rate of dissipation of TKE  $\varepsilon$ , and then infer the flux or eddy diffusivity [9]. Turbulence measurements can be made from a moored instrument [3], but in part as an attempt to obtain information about the spatial variability of the ocean turbulence, by far the most common approach is to use free-falling instruments that continuously record turbulent velocity and temperature fluctuations over the entire water column [9].

Figure 6 summarises measured turbulent dissipation rates made with a vertically-descending turbulence microstructure profiler, dropped 120 times over two consecutive tidal cycles at one location in 100m water depth on the NWS, just offshore from Port Hedland [4]. The site is known to very actively stirred by propagating NLIWs [25]. Despite the highly unsteady nature of the forcing associated with the shoaling and breaking internal tide at the location, there appears to be an almost normal distribution with a mean around  $\varepsilon = 3 \times 10^{-8} \text{ m}^2 \text{ s}^{-3}$ . Using a hydrostatic ocean model of the internal tide, and a simple large-scale energy balance, [8] estimated  $\varepsilon = 5 \times 10^{-8} \text{ m}^2 \text{ s}^{-3}$ , surprisingly close to this measured mean value in Figure 6. Not surprisingly there is a very large range of instantaneous values in the measurements in Figure 6, ranging from  $10^{-9}$  to  $10^{-5} \text{ m}^2 \text{ s}^{-3}$  and reflecting the unsteadiness of the ocean turbulence in response to the unsteadiness of the forcing associated with the dominant M2 internal tide forcing.

The challenge is to not only to make these measurements, and with sufficient coverage in time and space to characterise the coastal ocean, but to convert these to estimates of the vertical diffusion coefficient for the density-stratifying species [9]. The traditional method [21] is to infer this vertical diffusivity  $K_\rho$  indirectly from dissipation using the deceptively simple formulation

$$K_\rho = \Gamma \frac{\varepsilon}{N^2} \quad (6)$$

where the strength of the density stratification is quantified by  $N = \sqrt{-(g/\rho)d\rho/dz}$ , and the coefficient  $\Gamma$  characterises the efficiency of mixing in the density stratified fluid.

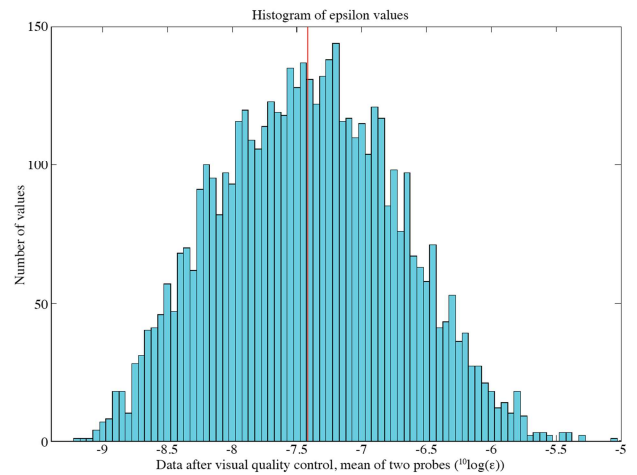


Figure 6. Measured rates of TKE dissipation  $\varepsilon$  on the NWS, where each estimate is for a 3 m vertical bin, from [4]. Red line denotes estimate of mean.

To illustrate, using an average from Figure 6 of  $\varepsilon = 3 \times 10^{-8} \text{ m}^2 \text{ s}^{-3}$ ,  $N = 7 \times 10^{-3} \text{ s}^{-1}$  (typical of mid-depth), and assuming  $\Gamma = 0.2$  (see below), equation (6) predicts  $K_\rho \approx 1 \times 10^{-4} \text{ m}^2 \text{ s}^{-1}$  or approximately  $10^3$  times the molecular diffusivity of heat, the stratifying species.

While common practice is to assume this efficiency  $\Gamma$  as fixed at 0.2, laboratory and DNS studies [9] and field measurements [3] suggest that, with the exception of the near-surface ocean thermocline region, this is likely an overestimate, by perhaps one to two orders of magnitude in diffusivities, and hence in  $K_\rho$ .

There thus remains fundamental questions in assessing the turbulent mixing, and these will likely only be answered by future direct measurements in the ocean at much higher turbulent Reynolds numbers than can be achieved in either laboratory or DNS simulations.

## Conclusions

The process of steepening of the linear internal (or baroclinic) tide in the coastal ocean can be described by well known analytical models for small amplitude waves, and with fully nonlinear and nonhydrostatic models for large amplitude waves. As seen on the NWS, for example, the connection between model and observations is challenging. As the ocean is in motion due to background motion forced by the barotropic tide itself, as well as other motions completely independent of the tide, even such fundamental issues as the propagation of the tide can be challenging to quantify. The fundamental parameter of importance here is the Froude number formed from the comparison of the (typically) non-linear internal wave speed and

the total background velocity. When the two are comparable, as happens on the NWS, the propagation of the tide and the arrival of internal tidal packets are not predicted by simple statistical methods. The turbulence driven by this forcing is, as a consequence, highly time-dependent as well as depth dependent due to the varying intensity of the density stratification and uncertainties around the efficiency of internal mixing. Recent measurements in the field which link knowledge of the background unsteady flow field with the observed turbulence intensities are, however, the key towards the development of robust numerical models capable of describing and even forecasting these dynamic processes in the coastal ocean.

### Acknowledgments

This work involves a number of collaborators, thanks in particular to Nicole Jones and Cynthia Bluteau at UWA, Oliver Fringer and Bing Wang at Stanford University, Bruce Sutherland at University of Alberta, and Leon Boegman at Queens University. The work has been supported by the Australian Research Council, the West Australian Marine Science Institute and Woodside Energy.

### References

- [1] Boegman, L. & Ivey, G.N. Flow separation and resuspension beneath shoaling nonlinear internal waves. *J. Geophys. Res. Oceans*, **114**, 2009, doi:10.1029/2007JC004411, 1-15.
- [2] Boegman, L., Ivey, G.N. and Imberger, J. The energetics of large-scale internal wave degeneration in lakes. *J. Fluid Mech.*, **531**, 2009, 159-180.
- [3] Bluteau, C.L., Jones, N. L. & Ivey, G.N. Turbulent mixing efficiency at an energetic ocean site, *J. Geophys. Res. Oceans*, **118**, 2013, doi:10.1002/jgrc.20292, 1-11.
- [4] Bluteau, C.L., Jones, N. L., Ivey, G.N. & Book, J. Turbulence and mixing under shoaling NLIW, *J. Geophys. Res. Oceans*, 2014, in prep.
- [5] Cacchione, D.A., Pratson, L.F. & Ogston, A.S. The shaping of continental slopes by internal tides. *Science*, **296**, 2002, 724-727.
- [6] Fringer, O.B., Gerritson, M. & Street, R.L. An instructed-grid, finite-volume, nonhydrostatic parallel coastal ocean simulator. *Ocean modelling*, **14**, 2006, 139-173.
- [7] Fringer, O.B., Ivey, G.N., Wang, B.J, Jones, N.L. and Bluteau, C.L. The formation, evolution and dissipation of nonlinear internal solitary waves. *J. Geophys. Res. Oceans*, 2014, in prep.
- [8] Holloway, P.E. A regional model of the semidiurnal tide on the Australian North West shelf. *J. Geophys. Res. Oceans*, **106**, 2001, 19,625-19,638.
- [9] Ivey, G.N., Winters, K.B. & Koseff, J.R.. Density Stratification, turbulence, but how much mixing? *Ann. Rev. Fluid Mech.*, **46**, 2008, 231-54.
- [10] Jackson, C.R., Da Silva, J.C.B. & Jeans, G. The Generation of Nonlinear Internal Waves.. *Oceanography*, **25**, 2012, 108-123.
- [11] Jacobs, D. The global market for Liquefied Natural Gas (LNG), *Res. Bank of Aust. Bull.*, **Sept**, 2011, 17-27.
- [12] Jones, N. & Ivey, G.N., Internal waves, *Encycl. Mar. and Offshore Eng.*, 2014, to appear.
- [13] Kaartvedt, S., Klevjer, T.A. & Aksnes, D.L. Internal wave-mediated shading causes frequent vertical migrations in fishes. *Mar. Ecol. Prog. Ser.*, **452**, 2012, 1-10.
- [14] Klymak, J.M. & Moum, J.N. Internal solitary waves of elevation advancing on a shoaling shelf. *Geophys. Res. Lett.*, **30**, 2003, doi:10.1029/2003GL011770, 1-4.
- [15] Lamb, K. Internal wave breaking and dissipation mechanism on the continental slope/shelf, *Ann. Rev. Fluid Mech.*, **46**, 2014, 231-54.
- [16] Lim, K., Ivey, G.N. & Jones, N.L.. Experiments on the generation of internal waves over continental shelf topography. *J. Fluid Mech.*, **663**, 2010, 385-400.
- [17] Martini, K.I., Alford, M.H., Kunze, E., Kelly, S.M. & Nash, J.D. 2012. Internal Bores and Breaking Internal Tides on the Oregon Continental Slope. *J. Phys. Oceanogr.*, **43**, 2012, 120-139.
- [18] Mathis, R., Marusic, I., Cabrit, O., Jones, N.L., Ivey, G.N. Modelling bed shear-stress fluctuations in a shallow tidal channel. *J. Geophys. Res. Oceans*, **119**, 2014, doi: 10.1002/2013JC009718, 1-15.
- [19] Nash, J.D., Alford, M.H., Kunze, E., Martini, K. & Kelly, S. Hotspots of deep ocean mixing on the Oregon continental slope. *Geophys. Res. Lett.*, **34**, 2007, 1-4.
- [20] Osborne, A.R., Burch, T.L. & Scarlet, R.I. The influence of internal waves on deep-water drilling. *J. Petrol. Technol.*, **30**, 1978, 1497-1504.
- [21] Osborne, T.R. Estimates of the local rate of vertical diffusion from dissipation measurements, *J. Phys. Oceanogr.*, **10**, 1980, 83-89.
- [22] Quaresma, L.S., Vitorino, J., Oliveira, A. & Da Silva, J. Evidence of sediment resuspension by nonlinear internal waves on the western Portuguese mid-shelf. *Mar. Geol.*, **246**, 2007, 123-143.
- [23] Sutherland, B.R. 2010. *Internal gravity waves*, Cambridge Univ. Press, 2010
- [24] Sutherland, B.R., Barrett, K.J. & Ivey, G.N. Shoaling internal solitary waves. *J. Geophys. Res.*, **118**, 2013, 4111-4124.
- [25] Van Gastel, P., Ivey, G.N., Meuleners, M.J., Antenucci, J.P. & Fringer, O.B. The seasonal variability of the large-amplitude internal wave field on the Australian North West Shelf. *Cont. Shelf Res.*, **29**, 2009, 1373-1383
- [26] Vlasenko, V., Stashchuk, N. & Hutter, K. *Baroclinic tides*, Cambridge Univ. Press, 2005
- [27] Zhang, Z., Fringer, O.B. & Ramp, S.R. Three-dimensional, nonhydrostatic numerical simulation of nonlinear internal wave generation and propagation in the South China Sea. *J. Geophys. Res. Oceans*, **116**, 2011, doi:10.1029/2010JC006424, 1-26.
- [28] Zhang, Z., Lowe, R., Falter, J. & Ivey, G.N. A numerical model of wave-and-current-driven nutrient uptake by coral reef communities *Ecol. Mod.*, **222**, 2011, 1456-1470.